TESI DI DOTTORATO IN EMATO-ONCOLOGIA E MEDICINA INTERNA CLINICO TRASLAZIONALE

Tutor: Prof. A. Nencioni

Dottoranda: Marzia Sucameli

Titolo della tesi: **Antioxidant and Antiviral potential against SARS-CoV-2 of cit-**2 **rus limonoids isolated from Grapefruit Seed Extracts**

Abstract:

The COVID-19 pandemic represented an unprecedented global emergency. Despite all efforts, COVID-19 remains a threat to public health, due to the complexity of mass vaccination programs, the lack of effective drugs, and the emergence of new variants. A link has recently been found between the risk of developing a severe COVID-19 infection and a high level of oxidative stress. In this context, we have focused our attention on natural compounds with the aim of finding molecules capable of acting through a dual antiviral / antioxidant mechanisms. In particular, we studied the potential of grapefruit seed extracts (GSE) and their main components, belonging to the class of limonoids. Using several physical and biological approaches including isolation and purification of GSE, oxidative and viability and antiviral assays, we have shown that extracts, particularly extract components belonging to the class of limonoids, are endowed with remarkable virucidal, antioxidant and mitoprotective activity.

1. Introduction

Coronaviruses (CoVs) are large positive stranded enveloped RNA viruses that generally cause enteric and respiratory diseases in humans and in animals. Most human CoVs have recently attracted global attention to their lethal potential and great infectious capacity. A highly pathogenic CoV, called SARS-CoV-2, dramatically emerged in December 2019 in Wuhan, China and has rapidly spread around the world the COVID-19 pandemic. SARS- CoV-2 infection and the destruction of lung cells triggers a local immune response, recruiting macrophages and monocytes that respond to the infection, release cytokines and an excessive amount of reactive oxygen species (ROS) is produced in various tissues. All people during viral infections are affected by chronic oxidative stress influencing the disease pathogenesis, inflammatory response, as well as organ and tissue dysfunction [1]. There are several common links between the risk of developing a severe COVID-19 infection and a high level of oxidative stress. In fact, a number of major risk factors related to COVID-19 severity and mortality have been identified: older age, hyperglycemia, hypertension, and obesity [2], factors strongly associated with increased oxidative stress [3, 4]. In addition, several *in vitro* and *in vivo* studies have shown that some viruses alter the redox balance of a cell to survive [5-7]. Furthermore, the prolonged clinical consequences linked to COVID-19 have recently been analyzed [8]. Controlling the oxidative stress response may be as important as targeting the virus. Therapies inhibiting viral infection (antiviral) and regulation of dysfunctional immune responses and oxidative stress may synergize to block pathologies at multiple steps. It

can be assumed that the high level of oxidative stress aggravates the prognosis of COVID-19, while the supplementation of antioxidants could reduce complications related to infection [9]. Diverse vaccines are being developed to treat COVID-19. According to the World Health Organization (WHO), more than 108 vaccine candidates were under clinical evaluation [10]. However, a certain portion of population cannot benefit of the vaccine. On the other hand, the real efficacy and safety of current therapeutic approaches will need further scrutiny when an adequate number of clinical data become available. Updated reports about the COVID-19 disease management have targeted its structure, pathology, and mechanism in order to have the best treatment. Food and Drug Administration (FDA) has created a special emergency program for possible coronavirus therapies, the Coronavirus Treatment Acceleration Program (CTAP). The program uses every available method to move new treatments to patients as quickly as possible, while at the same time finding out whether they are helpful or harmful. Currently, just one treatment was authorized COVID-19 and 11 treatments for emergency use were authorized by the Emergency Use Authorization (EUA) authority. In this context, small molecules acting on a specific viral target may represent potential tools to contrast this and future viral threats. Nature-derived bioactives (NDBs) have been used throughout the history as traditional medicines and many clinically used drugs have been inspired by natural products, which constitute a broad biodiversity of molecules, naturally selected over millennia of evolution. Several NDBs are able to counteract oxidative stress [1-4] also presenting an antiviral viral effect [11-15]. Recently, Prasansuklab and coworkes reviewed potential anti-viral natural

compounds with multiple targets related to coronaviruses. The research opened future prospective about some classes of natural compounds [11]. Most of the active molecules showed the inhibition of the enzyme Mpro in millimolar concentration [12-15].

Grapefruit seed extract (GSE) is well known for its antimicrobial properties. In a recent study, the effect of GSE has been evaluated on avian influenza virus (AIV), Newcastle disease virus (NDV) and infectious and bursal disease virus (IBDV). GSE has showed virucidal activity against AIV and NDV, namely enveloped viruses, however it was not able to show virucidal activity against the non-enveloped virus IBDV [17]. Notwithstanding these promising evidence, to date there are a few studies addressing the antiviral activity of GSE, and, to the best of our knowledge, no report on the activity of GSE against SARS-CoV-2. Moreover, recent studies suggested that GSE has antioxidant capacity [18,19]. Lipiński and collaborators confirmed that GSE could exert antioxidant activities by improving serum SOD, GSH-PX, T-AOC and CAT and decreasing serum MDA. This means that GSE can be an effective antioxidant, which could reduce reactive free radicals and oxidative stress by activating the antioxidant enzyme system [20]. Furthermore, GSE has a high growth inhibition effect against Gram-negative bacteria, such as Pseudomonas aeruginosa and *Escherichia coli*, as well as Gram-positive bacteria, such as *Staphylococcus* spp. and *Enterococcus* spp. [21,23]. Due to its high bactericidal effect and its safety, the extract is widely used in the food industry to retard or reduce bacterial growth, thus extending shelf-life of food [14]. Despite the vast literature, the mechanisms of action of GSE are only partly understood, and further investigations are warranted in order to

establish the molecular targets responsible of the antioxidant and antiviral proprieties. Intrigued by the possibility of having a safe and easily accessible natural extract in the arsenal of weapons against COVID-19, we planned to investigate the ability of the grapefruit seed extract (GSE) to counteract SARS-CoV-2 infection by studying both the potential antiviral effect as well as the ability to reduce uncontrolled oxidative stress response.

In this work, I present the results of our efforts. Starting from grapefruit seeds, we have generated a small collection of extracts, enriched fractions, and single molecules, which have been fully chemically characterized. All fractions and single components were evaluated for their virucidal and antioxidant activities. The collected results evidence that the most active constituents are terpenoids belonging to the family of limonoids and flavonoid glycosides.

2. Materials and Methods

2.1 Chemicals and Equipment

All solvents (acetonitrile, hexane, ethyl acetate, dichloromethane, ethanol, n-heptane, n-butanol, acetone, $CDCl_3$, CD_3OD) were obtained from Sigma-Aldrich (Milan, Italy). Isolation and purification of the compounds were performed by flash column chromatography on silica gel 60 (230–400 mesh). Analytical TLC was conducted on TLC plates (silica gel 60 F254, aluminum foil). Compounds on TLC plates were detected under UV light at 254 and 365 nm or were revealed by solution of anisaldehyde (2%) and H_2SO_4 (2%) in EtOH. NMR spectra were recorded on 600 MHz spectrometer Bruker Avance. High Resolution Electrospray Mass Spectra were acquired with Q-TOF Synapt G2 Si (WATERS), available at COSPECT Unitech Platform (Milan, Italy). HPLC analyses were performed with a liquid Chromatograph Varian ProStar, equipped with a ternary pump with a UV-Vis detector Varian Model 345. A RP 18 (Hypersil ODS, Thermo, 5 μm 300x4 mm i.d.) was used. All the sample were dissolved in ACN:H_2O 3:7 and filtered with 0.45 μm nylon filters. The elutions were performed with ACN and Water milliQ, flow 1 mL/min, λ 210 and 280 nm. The condition used were the following: t 0-15 min from ACN 10% to 60%; t 15-40 min ACN 60%.Preparative HPLC was performed with a C-18 Ascentis, Supelco (21.2 i.d. × 250 mm, 5 μm), fitted to a 1525 Extended Flow Binary HPLC pump and a Waters 2489 UV/Vis detector (both from Waters, Milan, Italy). The separation was performed in gradient condition: t 0-30 min from ACN 10% to 30%, at a flow rate of 15 mL/min, monitoring the eluate at 210 nm.

2.2 Plant Material and Extractions

Citrus paradisi seeds were collected during the summer 2020 in Cefalù, Contrada Parandola, Sicily. For hot air-drying was used a dryer (RGV Digital Dried) at 40 °C (water loss 64 %) until constant weight of grapefruit seeds. Dried seeds were grinded, and the powder (20 g) was sequentially extracted in the dark for 48 h at room temperature with hexane (2 × 100 mL) to remove the fatty matter, yielding **GSE1**, dichloromethane (2 × 100 mL) to give extract **GSE2**, and ethanol/water 1:1 (100 mL) to give extract **GSE3**. All the extracts were filtered and evaporated under reduced pressure to afford **GSE1** (10.0 g), **GSE2** (0.8 g), and **GSE3** (5.4 g) and analyzed by HPLC. Preliminary antiviral activity evaluation evidenced **GSE3** as the most active fraction (see discussion paragraph).

2.3 Isolation and purification

The hydroalcoholic extract (**GSE3**, 3.1 g) was dissolved in 100 mL of H_2O and extracted with n-BuOH (3 × 30 mL). The two phases in turn were dried under reduced pressure to give fractions $\mathbf{GSE3_{H20}}$ (2.4 g) and $\mathbf{GSE3_{BuOH}}$ (0.62 g) and analyzed by HPLC. $\mathbf{GSE3_{BuOH}}$ was purified by silica gel column chromatography using a mixture of EtOAc:Acetone:H_2O:HCOOH (8:1:0.5:0.5 and 7:2:0.5:0.5) as eluent. Two main fractions were isolated, **F1** containing a mixture of three limonoids and **F2** containing a mixture of two flavonoid glycosides. Fraction **F1** (45 mg) was subjected to silica gel column chromatography with hexane:EtOAc (3:7) to yield three fractions: obacunone (**1**) (4 mg), limonin (**2**) (30 mg), nomilin (**3**) (7mg). Fraction **F2** (35 mg) was purified

by preparative HPLC to yield narirutin (**4**) (4.8 mg, rt 17.30 min) and naringin (**5**) (2.1 mg, rt 18.15 min). The structures of the isolated limonoid and glycoside flavonoid were confirmed by 1D and 2D NMR and MS experiments. Complete structural characterization of compounds is provided in Supporting Materials.

2.4 Optimization of extraction procedure

Once identified the most active compounds, alternative extraction protocols were investigated: 1) ethanol extraction (EtE), 2) acetone/ethyl acetate extraction (AAE) and 3) triphasic extraction (TE). For ethanol extraction (EtE), grapefruit seeds powder (3 g) was stirred with EtOH (10 mL 2) at rt in the dark for 48 h. The extracts were filtered and evaporated under reduced pressure. For acetone/ethyl acetate extraction (AAE), grapefruit seeds powder (3 g) AAE was performed with a mixture 1:1 (10mL 2) at rt in the dark for 48 h. The extracts were filtered and evaporated under reduced pressure. For triphasic extraction (TE), grapefruit seeds powder (3 g) was stirred with a system of five solvents with different polarity (n-Eptane/EtOAc/ACN/ButOH/H_2O with proportion 22:14:29:8:27). This mixture was selected, being the most efficient for the model of natural products reported by Gori et al [24]. The mixture was stirred for 14 h at 35 °C and decanted. The three-phasic solvent system was filtered, separated by a separatory funnel and evaporated under reduced pressure. Pure limonin and nomilin were used as standards for quantification by HPLC analyses of extracts. Limonin and nomilin content in the crude extract were determined by high-performance liquid chromatography (HPLC). The retention time was 15.68 min for

limonin (**2**), 16.49 min for nomilin (**3**), and 17.35 min for obacunone (**1**). A linear correlation between limonin and nomilin concentration and area of peaks was obtained for the covered concentration ranges from 0.11 to 1.75 μg/ml, sustained by the regression coefficient (R^2 = 0.9932 and 0.9310 respectively) (figure1).

2.5 Cell cultures

A549 (Lung epithelial) cells were cultured in T25 tissue culture flasks. RPMI Medium was used, supplemented with 10% fetal bovine serum (FBS), 100 U/ml penicillin and 100 U/ml streptomycin and 2 mM L-glutamine in a humidified atmosphere of 95% air and 5% CO2 at 37 °C. Vero E6 (Cercopithecus aethiops derived epithelial kidney, C1008ATCC CRL-1586) cells were grown in Minimum Essential Medium (MEM + GlutaMAX, Gibco) supplemented with 10% Fetal Calf Serum (FCS), 100 U/ml penicillin, 100 U/ml streptomycin, 1 mM sodium pyruvate, and 1% non-essential amino acids.

2.6 Cell viability and cell morphology

For dose-dependent assay, A549 cells were treated with 10, 100 and 300 μg/ml of extracts for 24 hours. Cells were grown at a density of $2x10^4$ cell/well on 96-well plates in a final volume of 100 μl/well. After treatments, the cell viability was measured by MTS assay (Promega Italia S.r.l., Milan, Italy). MTS was utilized according to the manufacturer's instructions. After cell treatments, the incubation was continued for 2 hours at 37 °C in 5% CO_2. The absorbance was read at 490 nm using the Microplate Reader GloMax fluorimeter (Promega Corporation, Italy). Cell

viability was expressed as arbitrary units of absorbance, with the control group set to 1 (Figure S1). For cytotoxicity analysis, Vero E6 cells were grown at a density of $1x10^4$ cell/well in 96-well plates and were treated for 24 h with semi-log dilutions of **GSE3**, **GSE3$_{n\text{-}BuOH}$**, obacunone (**1**), limonin (**2**) and nomilin (**3**) (from 0,5 mg to 0,125 mg). Then, 5 ml of tetrazolium salt XTT (Cell Proliferation Kit II, Roche) was added to the cells and 10% of Electron-Coupling Reagent was added, according to the manufacturer's instructions. After incubating for 2 h at 37 °C, plates were read in a spectrophotometer at 450 nm. After this incubation period, the formazan dye formed was quantified using a scanning multi-well spectrophotometer. The measured absorbance directly correlates to the number of viable cells.

2.7 Analysis of Reactive Oxygen Species (ROS)

For oxidative stress generation 500 µM of tert-butyl hydroperoxide (Luperox® TBH70X, Merck Life Science S.r.l., Italy) was used for 2 hours, alone and in combination with grapefruit seeds extracts treatment. The control (Ctrl) groups received an equal volume of the medium. For the DCFH-DA, and JC-1 assays the extract was utilized at 100 µg/ml for 2 hours. The treated and control cells were analyzed by using microscopy (Axio Scope 2 microscope; Zeiss, Germany). At the end of the treatments, each sample was added DCFH-DA (100 µM) and placed in the dark for 10 min at room temperature. After washing with PBS, cells were analyzed using a Microplate Reader GloMax fluorimeter (Promega Corporation, Italy) at the excitation wavelength of 475 nm and emission wavelength 530 nm for fluorescence intensity detection and results were expressed as a percentage of the control group. Cells fluorescence was also visualized

using the fluorescence microscope Zeiss Axio Scope 2 microscope (Carl Zeiss, Oberkochen, Germany).

2.8 Mitochondrial membrane potential analysis

The mitochondrial transmembrane potential was measured by plating and treating the cells as mentioned above. After treatment, the cells were incubated for 30 min at 37°C with 2 μM JC-1 red dye (5,5′,6,6′-tetrachloro-1,1′,3,3′-tetraethylbenzimidazolylcarbocyanine iodide) using the MitoProbe JC-1 assay kit (Molecular Probes, USA). Fluorescence emission shift of JC-1 from red (590 nm) to green (529 nm) was evaluated by the fluorescence microscope equipped with a 488 nm excitation laser using the Microplate Reader GloMax fluorimeter (Promega Corporation, Italy).

2.9 Mitochondrial morphology analysis

Cellular mitochondria were stained using the MitoTracker Deep Red (Invitrogen, Carlsbad, CA, USA) dye (20 nM) for 15 min, washed twice with growth medium, and observed under the fluorescence microscope (488 nm excitation/ 590 nm emission). Original fluorescence images were converted to binary images. Mitochondrial shapes were obtained by visualizing the mitochondria outlines automatically drawn by the ImageJ software (Public Domain, BSD-2 license, National Institutes of Health, Bethesda, MD, USA). Morphometric mitochondria data, length and perimeter, were calculated from each mitochondrial outline (N 500).

2.10. Virus propagation

Viral isolate BetaCov/Italy/CDG1/2020|EPI ISL 412973|2020-02-20 (GISAID accession ID: EPI_ISL_412973), obtained from a COVID-19 patient, was propagated by inoculation of 70-80% confluent Vero E6 cells in 75 cm^2 cell culture flasks. Cells were observed for cytopathic effect (CPE) every 24 h. Stocks of SARS-CoV-2 virus were harvested at 72 h post infection, and supernatants were collected, clarified, aliquoted, and stored at −80 °C. Infectious virus titer was determined as Plaque Forming Units (PFU/ml). Virus propagation was conducted under biosafety level (BSL) 3 facilities at ISS (Rome, IT).

2.11. Plaque Reduction Neutralization Test

The method used for Plaque Reduction Neutralization Test (PRNT) was previously described [25]. The GSE compounds were resuspended in 30% dimethyl sulfoxide (DMSO) leading to a final concentration of 1 mg/ml that did not affect the growth of the cells in *in vitro* experiments. Then serial 2-fold dilutions of GSE extracts (from 0.5 mg/ml to 0.015 mg/ml) were incubated with 80 PFU of SARS-CoV-2 at 4 °C overnight. The mixtures were added in triplicates to confluent monolayers of Vero E6 cells, grown in 12-well plates and incubated at 37 °C in a humidified 5% CO_2 atmosphere for 60 min. Then, 4 ml/well of a medium containing 2% Gum Tragacanth + MEM 2X supplemented with 2.5% of heat-inactivated FCS were added. Plates were left at 37°C with 5% CO_2. After 3 days, the overlay was removed, and the cell monolayers were washed with PBS to completely remove the overlay medium. Cells were stained with a crystal violet 1,5% alcoholic solution. The presence of SARS-CoV-2 virus–infected cells was indicated by the formation of plaques. The half-maximal

inhibitory concentration (IC_{50}) was determined as the highest dilution of substance resulting in 50% (PRNT50) reduction of plaques as compared to the virus control. PRNT is a live neutralization assay that was conducted under biosafety level BSL3 facilities at ISS.

2.12 Statistical Analysis

The significance of the differences in the mean values was evaluated by using one-way analysis of variance (ANOVA) followed by Bonferroni's post hoc test. Differences were considered significant when the value was $p \leq 0.05$. Standard deviation (SD) of SARS-COV-2 reduction in infectivity was calculated at different concentration of each compound. In this study, 95% of confidence interval (CI) was considered.

3. Results

3.1 Chemical isolation and characterization

3.1.1 Isolation of bioactive compounds

A preliminary screening of the antiviral activity of extracts **GSE1** (hexane), **GSE2** (dichloromethane), and **GSE3** (ethanol/water 1:1) against SARS-CoV-2 showed that the most promising fraction was **GSE3** (see below for details). Thus, the efforts were focused on **GSE3**, the hydroalcoholic extract, to shed light on the molecules responsible for the activity. The extract was partitioned between water and n-butanol. The aqueous phase contained mainly carbohydrates, as showed ^{1}H-NMR, and resulted inactive in biological assays. The alcoholic phase (**GSE3$_{\text{n-BuOH}}$**) was purified by column chromatography on silica gel to obtain two main fractions. Further purifications were performed on **F1** and **F2**, as reported in scheme 1. The main isolated compounds belonged to the classes of limonoids and flavonoids. Obacunone (**1**) (0.2 mg/g DW), limonin (**2**) (1.4 mg/g DW), nomilin (**3**) (0.3 mg/g DW), narirutin (**4**) (0.6 mg/g DW) and naringin (**4**) (0.3 mg/g DW) were obtained as pure molecules (figure 1)

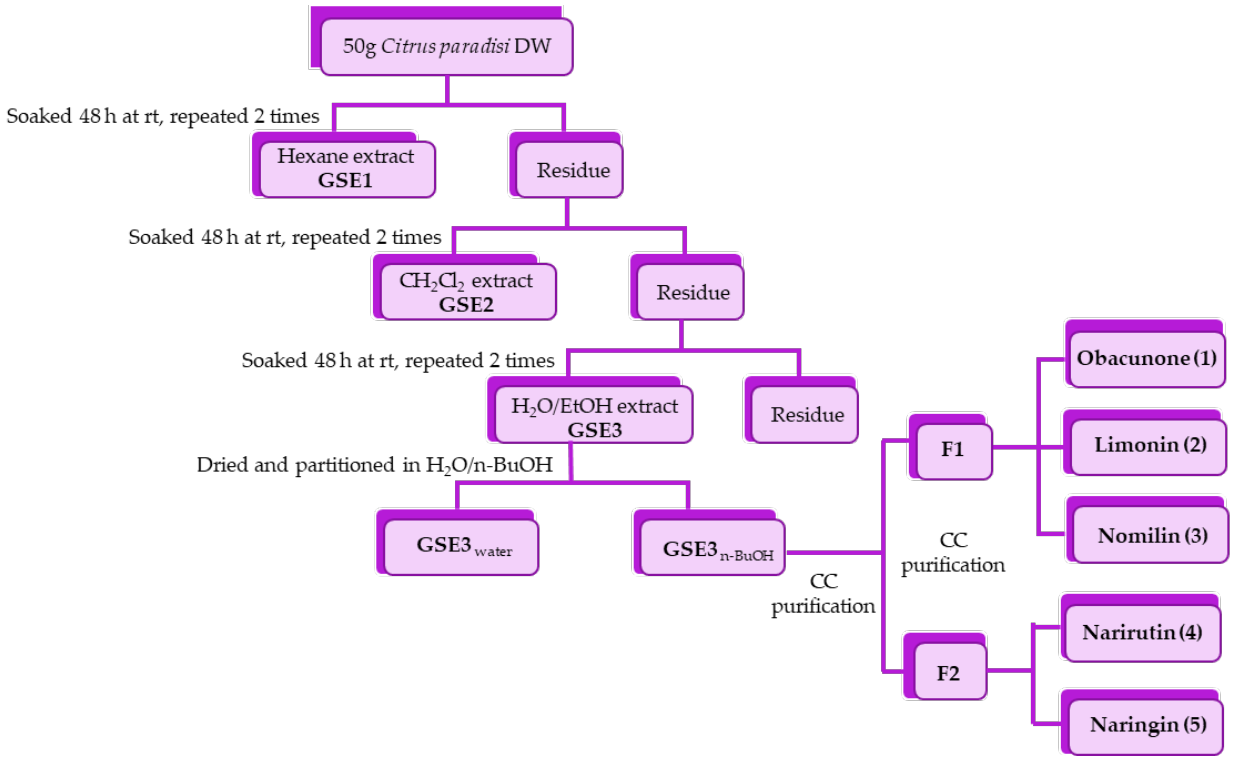

Figure 1. Schematic representation of the extraction process from *Citrus paradisi* seeds.

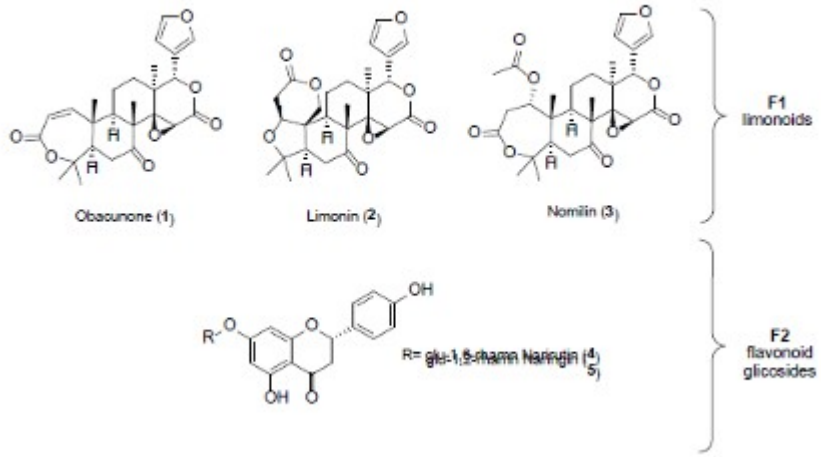

Figure 2. Structures of purified limonoids and flavonoid glycosides.

3.1.2 Comparison of extraction protocols

To optimize the yield of the most promising compounds (contained in the alcoholic fraction of the sequential extraction, SE), alternative extraction

methods were carried out: ethanol extraction (EtE), acetone/ethyl acetate extraction (AAE) and triphasic extraction (TE). The conditions and yields of all the extraction are reported in table S1 in supplementary materials. Briefly, using SE, it was found that the grapefruit seeds contained 26% of apolar compounds, like fatty materials; while the DCM (2%) and EtOH/H_2O (13%) extracts were composed of medium polar and polar compounds, like aglycons and glycosides of limonoids and flavonoids. EtE and AAE were also investigated, as they required a single extraction of green and sustainable solvents [26].

The total quantity of main limonoids (limonin and nomilin) in percentage with respect to the dried matrix (DW) was 10% and 20% in EtE and AAE, respectively (calculated on the bases of the areas in HPLC chromatograms). The yield of EtE extraction (9.19 mg/g) was comparable to SE (DCM + EtOH/H_2O, 9.49 mg/g). Conversely, the acetone/EtOAc extract was richer of limonoids than GSE (20.26 mg/g). Despite an efficient capability of limonoid extraction by these two eco-friendly approaches, the presence of large amount of fatty acids was deleterious for the purification and isolation of pure compounds.

To maintain an exhaustive quality of the extract, significantly reducing the presence of primary metabolites, we employed the triphasic method (TE) for the extraction of grapefruit seeds. The triphasic extraction had the advantage of mixing five solvents with different polarities for a single extraction step, with a consequent process time and solvent consumption reduction. The solvents used for the TE were chosen on the bases of the results reported in the paper of Gori et al. [24]. The yields of extraction of

the apolar phase, intermediate phase and polar phase were 13%, 5% and 8%, and were composed largely of fatty materials, secondary metabolites and sugars, respectively, as showed by NMR spectra. This method resulted inconvenient, as limonoids were distributed in all the phases. Moreover, the purification step was not improved. A possible alternative to optimize the triphasic extraction of limonoids, could be the variation of mixture composition and/or ratios. The above reported results suggested that the best protocol for the extraction of active compounds in terms of yields of limonoids and purification efforts was the one based on the use of environmental friendly solvents acetone and ethyl acetate.

Table *1***.** Content of main limonoids (limonin and nomilin) in the extracts.

Extraction method	**Extract**	**Total LM content (mg/g DW ± SD)**
SE	GSE1-Hexane	-
	GSE2-DCM	5.43 ± 1.60
	GSE3-Ethanol/H_2O 1:1	4.05 ± 1.07
		9.48
EtE	EtOH	9.19 ± 1.34
AAE	Ac/AcOEt 1:1	20.26 ± 0.90
TE	Apolar phase	4.46 ± 0.22
	Intermediate phase	12.76 ± 1.25

	Polar phase	9.59 ± 1.04
		26.81

4.1 *Virucidal activity on SARS-CoV-2*

After a preliminary screening of **GSE1**, **GSE2** and **GSE3**, we choose to focus on **GSE3** and its main components, which showed the higher virucidal activity when used to treat the virus before its inoculum on Vero E6 monolayers. Their capacity to neutralize the authentic virus SARS-CoV-2 was evaluated in vitro through PRNT50, tested in triplicates and the concentration required to inhibit 50% of infection (IC_{50}) was used as cut-off threshold of virucidal acivity. A standard XTT viability assay was performed prior to the assessment of the virucidal activity of **GSE** to rule out the possibility that the compounds may have cytotoxic effects on the Vero E6 cells (see supplementary materials). As mentioned above, we focused on **GSE3**, the hydroalcoholic extract and on the molecules contained therein (Figure 1). A substantial difference was evidenced in the results obtained from tests on $\mathbf{GSE3_{n\text{-}BuOH}}$ and $\mathbf{GSE3_{water}}$. As Figure 3 reports, the rate of inhibition of $\mathbf{GSE3_{n\text{-}BuOH}}$ at 0,5 mg/ml settled over 70% as result of its virucidal activity, compared with a similar concentration of $\mathbf{GSE3}_{\boldsymbol{water}}$, that proved to be completely ineffective against SARS-CoV-2 (Figure 3A). The following dilution of 0,125 mg/ml is still effective, and the inhibitory effect fell below 50% at 0,05 mg/ml (Figure 3B), with an IC_{50} of 0,118 mg/ml.

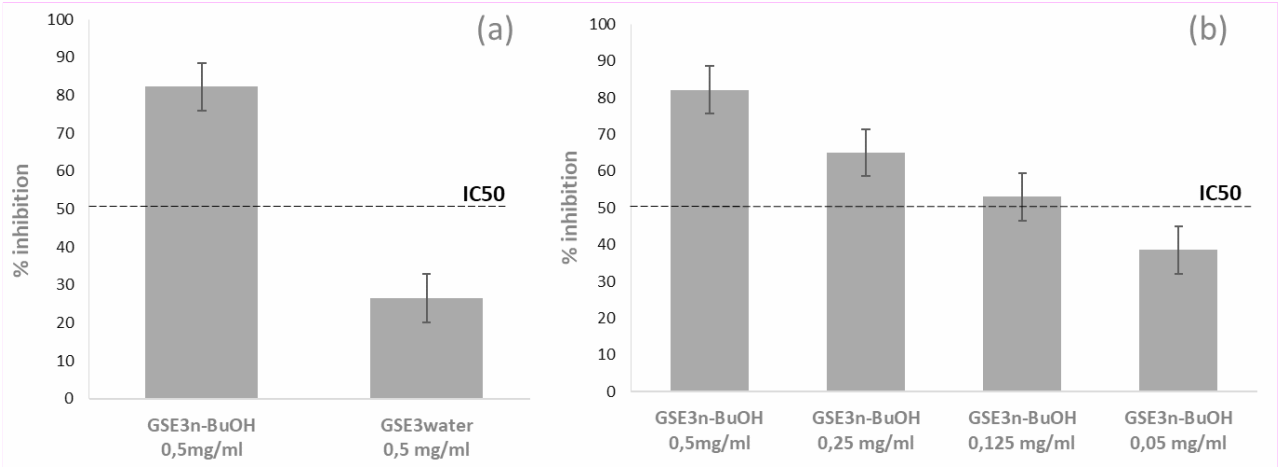

Figure 3: rate of inhibition by **GSE3$_{n\text{-}BuOH}$** and **GSE3$_{water}$** (a) and by **GSE3$_{n\text{-}BuOH}$** dilutions (b).

Beside **GSE3$_{n\text{-}BuOH}$** and **GSE3$_{water}$,** the single limonoids obacunone (**1**), limonin (**2**), nomiline (**3**) of **F1** fraction and F2 fraction containing narirutin (**4**) + naringin (**5**) were also tested against the virus. Results demonstrate that the components obacunone (**1**), limonin (**2**) and nomiline (**3**) were all effective against SARS-CoV-2 with IC_{50}s ranging between 15 and 31 µg/mL, as shown in Figure 4. The virucidal activity increases gradually as the extraction process goes further, from **GSE3$_{n\text{-}BuOH}$** to its single fractions of **F1**. No inhibitory effect has been shown by the fraction **F2** containing narirutin (**4**) + naringin (**5**).

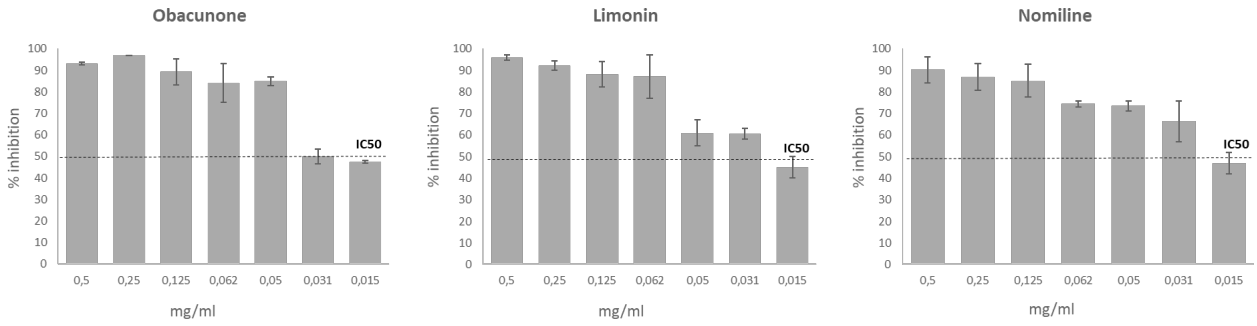

Figure 4: Dose-dependent inactivation of SARS-CoV-2 by **GSE3** enriched fractions obacunone (**1**), limonin (**2**), nomiline (**3**). Half-maximal inhibitory concentration threshold, IC_{50}, calculated showed.

5.1 Biological activity

5.1.1. Effect of grapefruit seeds extracts on cell viability

To evaluate the citocompatibility of the grapefruit seeds extracts, different concentrations of each estract or single pure molecule were added to lung epithelial cells - A459 for 24 hours and MTS cell viability assay was performed. Figure S2(a) (see supporting information) showed that no toxicity was detected at 0.01 and 0.1 mg/ml compared with the control. On the contrary, at 0.3 mg/ml, the extracts showed a decrease in cell viability and for this reason; this concentration was discarded for subsequent biological evaluations. The result was also confirmed by the morphological inspection of the cells treated at 0.1 mg/ml of extracts concentration (Figure S2(b)), where correct cell shape was observed, confirming the absence of any cell damage. The grapefruit seed extracts protective property was evaluated by treating cells with TBH 500 μM alone or in combination with increasing concentrations of the extracts and pure molecules after 2 hours of incubation. As detected by MTS assay, only nomilin (**3**) was able to inhibit TBH-induced toxicity at 0.1 mg/ml (Figure 6(a)). This result was also confirmed by microscopic observation in which a significant recovery of the altered cell morphology was observed (Figure 6(b)).

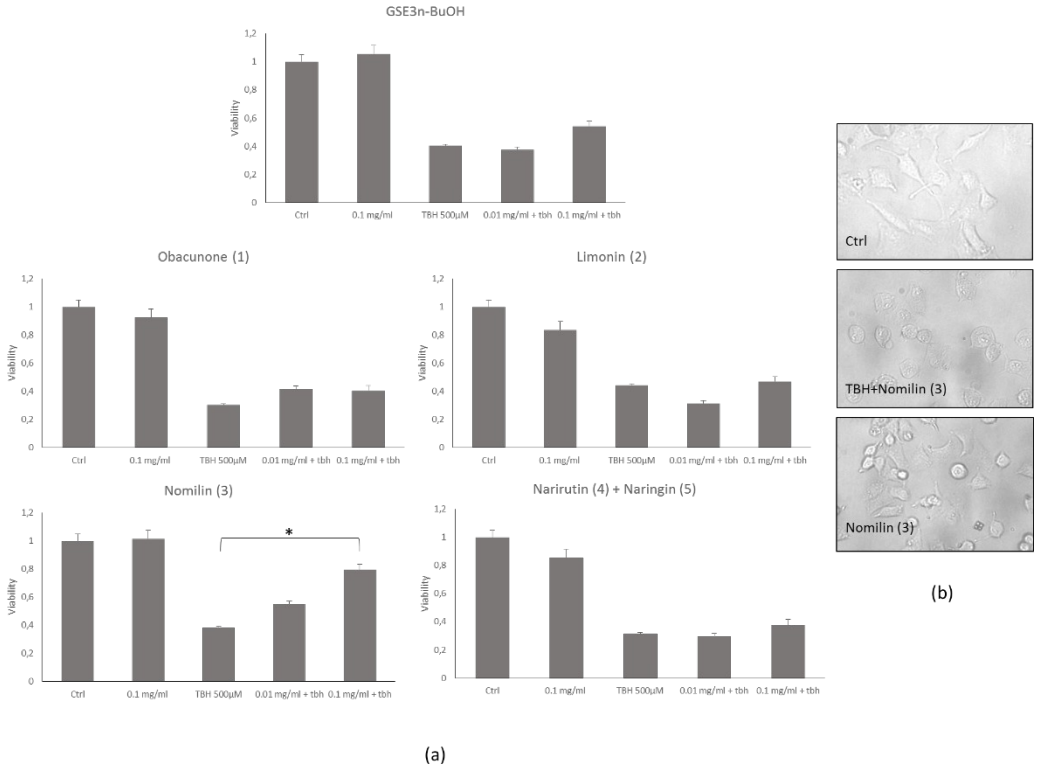

Figure 6. Grapefruit seeds extracts protect A549 cells from cellular damage. (a) Histograms of viability assay on untreated cells (Ctrl) or cells treated with TBH alone or with grapefruit seeds extracts at increasing concentrations for 2 hours. (b) Representative morphological images of untreated cells (Ctrl) or cells treated with TBH or cotreated with TBH and nomilin (**3**) at 0.1 mg/ml. * $p < 0.05$ as compared to treated (TBH) group.

5.1.2 Effects of grapefruit seeds extracts on ROS production induced by THB treatment

Grapefruit seeds extracts antioxidant ability was analyzed by using DCFH-DA assay. At 0.1mg/ml all extracts presented a moderate decreased of TBH-induced ROS generation. Notably, **GSE3$_{n\text{-}BuOH}$** decreased significantly TBH-induced ROS generation at 0.1 mg/ml. In particular,

nomilin (**3**) decreased significantly TBH-induced ROS generation at 0.01 and 0.1 mg/ml (Figure 7(a)). The result was also confirmed by fluorescence microscope inspection (Figure 7(b)), in which untreated, or nomilin (**3**) cotreated with TBH, did not show any fluorescence; in contrast, cells treated with TBH showed green fluorescence due to ROS generation. These results are in accordance with the effect of nomilin (**3**) on recovery the cellular viability treated by TBH (Figure 7(b)). Based on these data, the nomilin (**3**) dose chosen for subsequent protection experiment was 0.1 mg/ml.

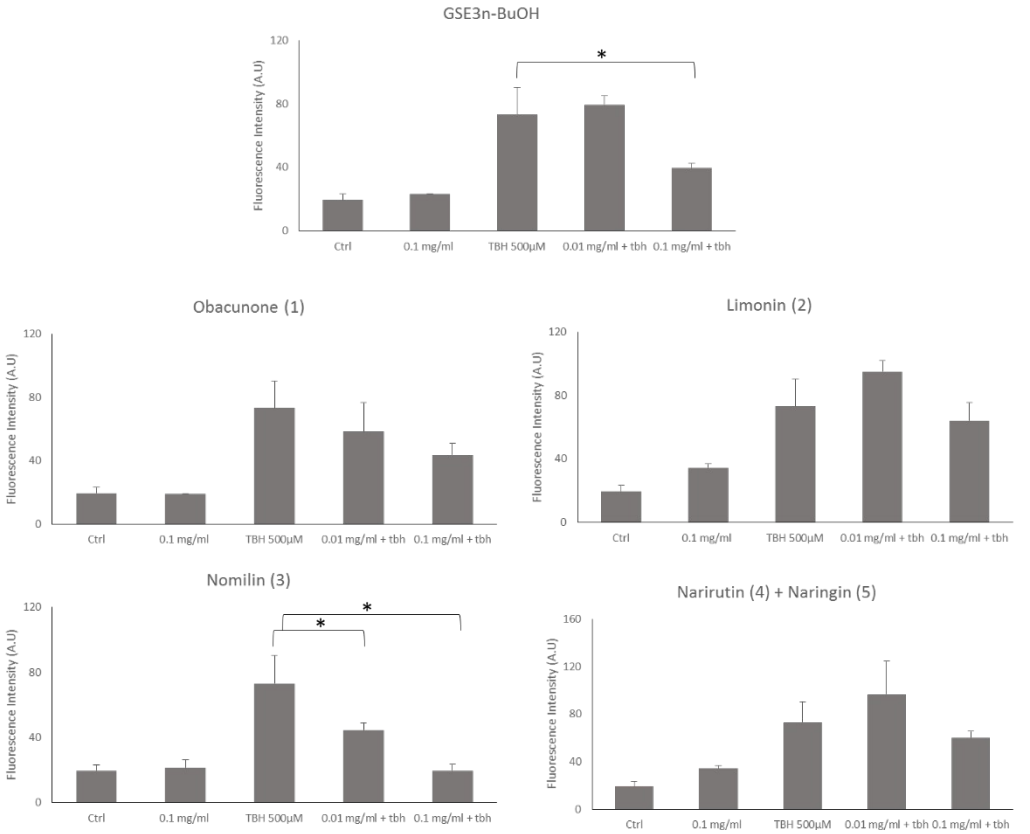

(a)

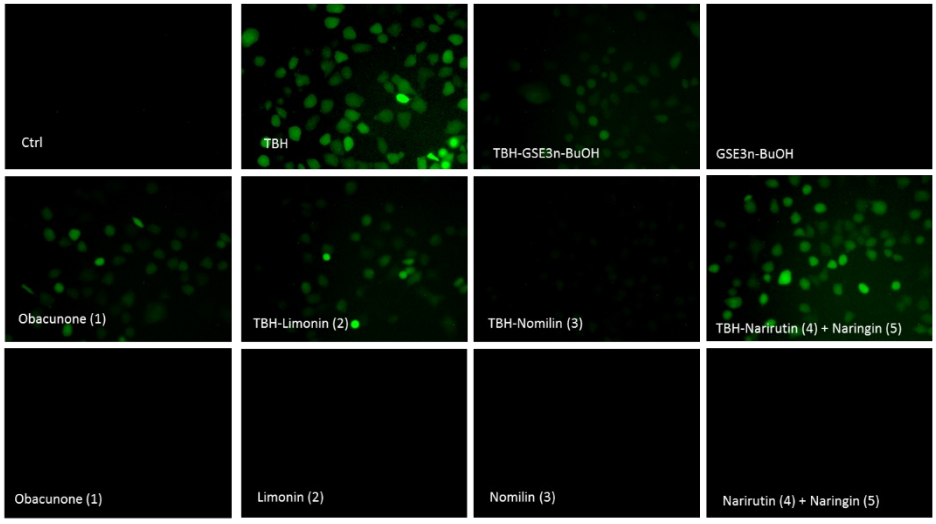

(b)

Figure 7. Grapefruit seeds extracts protects cells from oxidative stress. (a) Histogram of ROS generation of untreated cells (Ctrl) or cells treated with TBH alone or in cotreatment with extracts at increasing concentrations for 2 hours. (b) Representative cells fluorescence images of untreated cells (Ctrl) or cells treated with TBH or cotreated with TBH and grapefruit

seeds extracts 0.1 mg/ml and treated with the extracts at 0.1 mg/ml each. * $p < 0.05$ as compared to treated (TBH) group.

*5.1.3 Effects of nomilin (**3**) on mitochondrial membrane potential altered by TBH treatment*

Excessive ROS production alters mitochondrial components driving to the mitochondrial dysfunction. Based on the experiments previously performed, the potential protective effect of nomilin on mitochondrial dysfunction was evaluated. A549 cells treated with TBH at 500 μM for 2 hours showed an intense green fluorescence indicating that a high depolarization of the mitochondrial membrane occurred. Instead, cells cotreated with TBH and nomilin showed a higher red fluorescence emission similar to the untreated control (Ctrl) (Figure 8), clearly indicating a mitochondria protection effect of the limonoid.

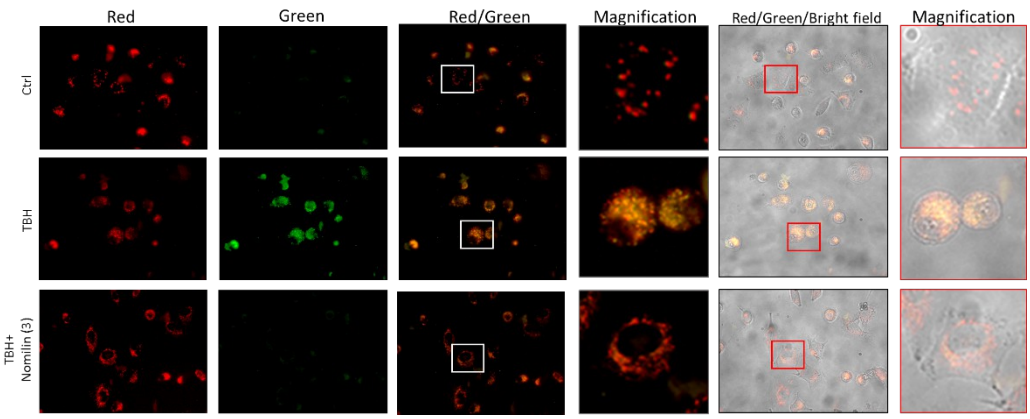

Figure 8. Grapefruit seeds extracts protect against mitochondrial damage. Fluorescence microscope images of cells untreated (Ctrl) or treated with TBH alone or with the nomilin (**3**) and submitted to JC-1 assay.

*3.5. Effects of nomilin (**3**) on mitochondrial morphology*

To analyze the mitochondria morphology, the A549 cells were stained with MitoTracker fluorescence dye. By microscopy fluorescence inspection the control was characterized by an interconnected mitochondrial network, with a tubular shape. Treatment of the cells with TBH resulted in a concomitant change in mitochondrial morphology from tubular networks to fragmented puncta (circular). When nomilin (**3**) was co-administered with the strong oxidizer TBH, the morphology and mitochondrial was partially recovered (Figure 9).

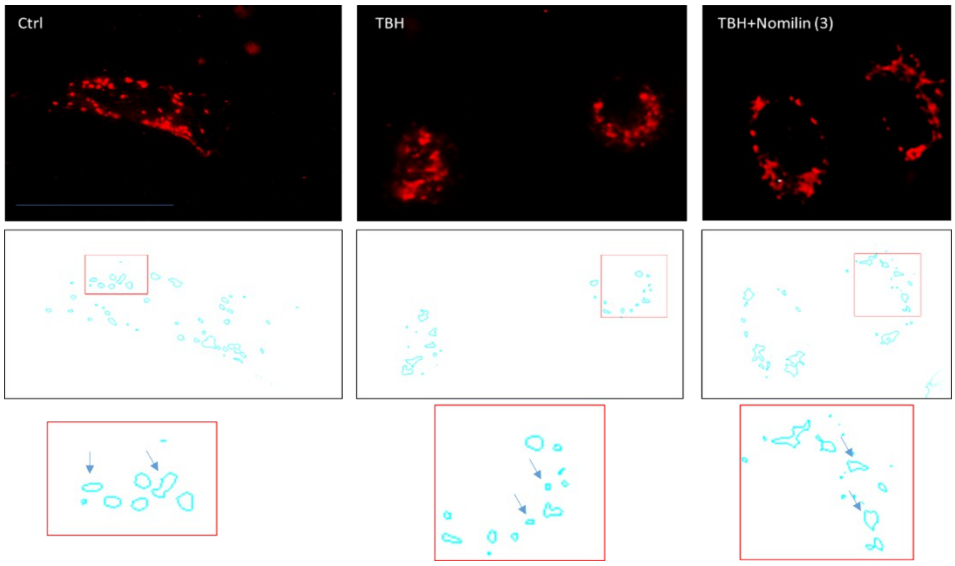

Figure 9. Representative fluorescence microscopy images of mitochondria stained with the MitoTracker Deep Red in untreated cells (Ctrl) or treated with TBH alone or in combination with nomilin (**3**).

4. Discussion

COVID-19 pandemic has represented an unprecedented global emergence. Countries have globally put a lot of efforts to counteract the epidemic by appropriate public health strategies, developing drugs and vaccines against SARS-CoV-2 [27,28].

Despite all the efforts, COVID-19 remains a public health threat, because of the complexity of mass vaccination programs, the lack of effective drugs and the emergence of new VOC (variants of concern). It has been recently found a link between the risk of developing a severe COVID-19 infection and a high level of oxidative stress. Thus, a regulation of dysfunctional immune responses becomes as important as therapies inhibiting viral infection to block SARS-CoV-2 related pathologies. In this context, we focused our attention on natural compounds with the aim of finding molecules able to act through a two-pronged antiviral/antioxidant mechanism. In particular, we investigated the potential of grapefruit seed extracts (GSE) and of their main components, belonging to the class of limonoids. Limonoids are natural tetracyclic triterpenoids widely distributed in the *Rutaceae* and *Meliaceae* families of the Citrus genus. These secondary metabolites can be found in several parts of plant, such as fruits, peels, root bark, roots, seeds, ect. [29] Limonoids are biosynthesized through isoprenoids pathway in the citrus seeds. [30] This class of molecules can be found in free or glycosidic form. The first one is collected during the development of tissues, while the concentration of the second form increases during the maturation of seeds. Grapefruit seeds show the highest limonoids content, limonin and nomilin being the most

abundant [31]. Various interesting biological activities of this class of compounds are reported, including antitumoral, anti-inflammatory, anti-obesity, anti-hyperglycemic, anti-oxidative, anti-neurological diseases, anti-insecticidal, antibacterial and antiviral activities [32–35]. Interestingly, a recent work by Vardhan et al., evidenced the potential antiviral activity of limonoids on the basis of *in silico* ADMET and molecular docking studies on the inhibition of five Sars-CoV-2 protein targets [36]. Intrigued by these findings, we carried out a sistematic evaluation of the antiviral activity against SARS-COV-2 of GSE extracts and purified single molecules, obtained by the development of an efficient extraction protocol from the natural matrix. The results confirmed that the most active compounds belonged to the family of limonoids.

In particular, component nomiline (**3**) and obacunone (**1**), showed the highest potency against virus (IC_{50} between 15 and 30 µg/mL) without any cytotoxic effects on the Vero E6 cells. It is interesting to note that the virucidal activity increases gradually following the extraction process from the GSE extract (IC_{50} >1.25 mg/ml) to the single molecules.

We analysed the antioxidants activity of the limonoids by in vitro experiments using the powerful oxidant TBH. We also investigated the cell viability, and ROS production induced by treatment of human lung epithelial cells with TBH in the presence of limonoids. Moreover, for the first time, we studied the effect of limonoids on the mitochondrial dysfunction. The mitochondrial dysfunction driven by oxidative stress was blocked by the treatment with nomilin (**3**), one of the isolated limonoids. Nomilin (**3**) inhibited the oxidative-induced mitochondrial membrane

damage, indicating that its radical scavenging effect is also extended to mitochondrial ROS. Taken together, these data indicate that only nomilin (**3**) exerts a protective role on the cell's central organelle, involved in several cellular activity.

5. Conclusions

In this work, we investigated natural extract of grapefruit seeds as a source of active molecules to fight against SARS-CoV-2 infection by a dual approach, involving both vir-ucidal and antioxidant activity. GSE extracts, in particular components of the extract be-longing to the class of limonoid, are endowed with significant virucidal, antioxidant and mitoprotective activity. More research will be needed to understand if this molecule will be considered as oral or nasal treatment of SARS-Cov-2 infection in the near future.

Entry	Solvents	Temperature	Time	Drug/solvent (g/mL)	Y
GSE1-3	Hexane	r.t.	24h (x2)	20/100	2
	DCM				2
	Etanol/H_2O 1/1				1
EtE	EtOH	r.t.	24h (x2)	3/10	1
AAE	Ac/AcOEt	r.t.	24h (x2)	3/10	2
TE	n-Heptane/AcOEt/ACN/ButOH/H_2O (22:14:29:8:27)	35°C	7h (x2)	3/53.4	1 p 5 d p 8

					p

In summary, targeting at the same time viruses and host-cell specific defense mechanism represents an original and advantageous approach for developing a broad-spectrum antiviral agent. This strategy is characterized by a lower risk of resistance acquisition and possibly will give us the instruments to counteract the present disease as well as future pandemics.

Supplementary Materials:

Table S1 condition and yields of all the extraction

Figure S1. Cells viability by XTT assay. Level of cytotoxicity of GSE3 (A) and GSE3 main components (B).

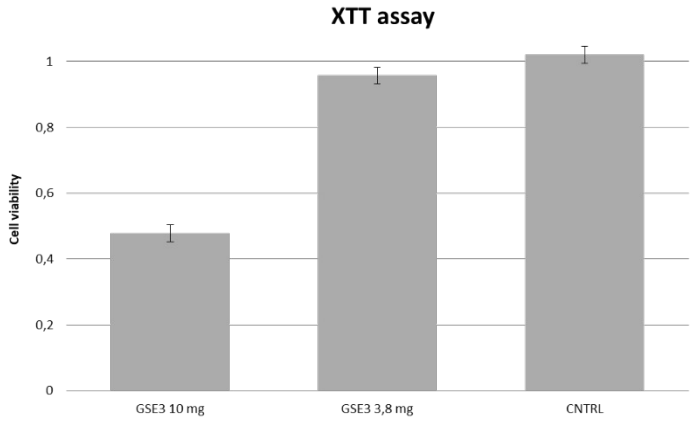

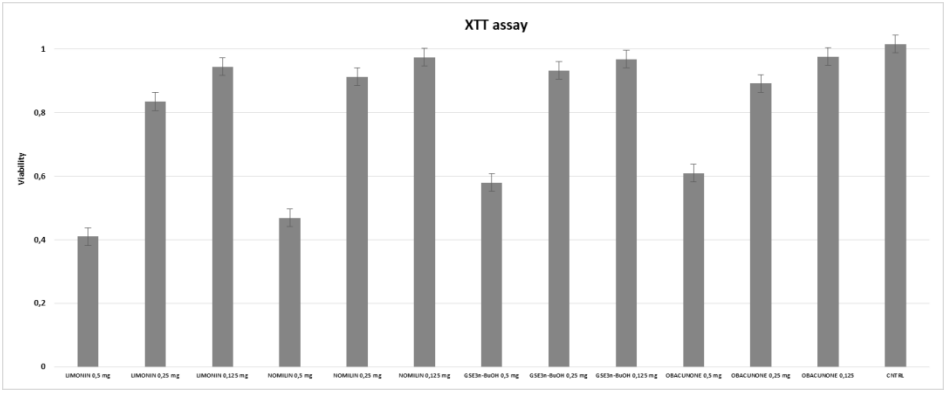

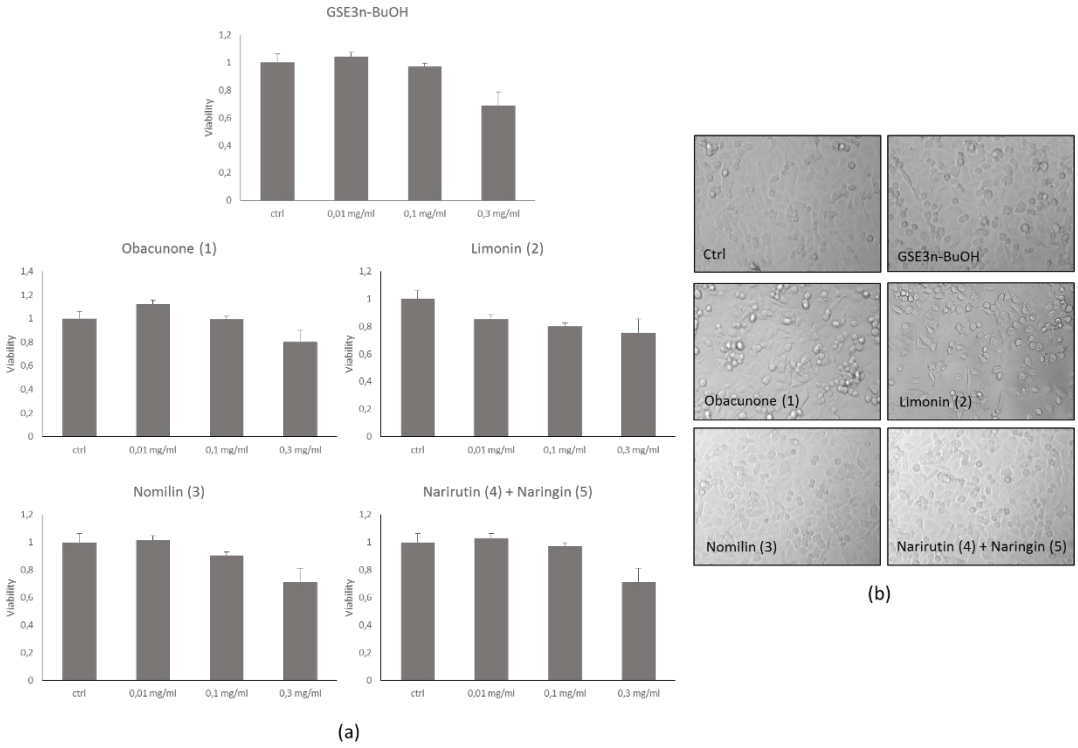

Figure S2. Cytotoxicity of the grapefruit seeds on A549 cells. (A) Histograms of MTS cell viability assay. (B) Representative morphological images of untreated cells (Ctrl) and after 24 hours from the addition of 0.1mg/ml of the extracts

References

1. Reshi, M.L.; Su, Y.C.; Hong, J.R. RNA Viruses: ROS-Mediated Cell Death. *Int J Cell Biol*. **2014**, 467452.

2. Williamson, E.J.; Walker, A.J.; Bhaskaran, K.; Bacon, S.; et al. Factors associated with COVID-19-related death using OpenSAFELY. *Nature*. **2020**, *584*, 430-436.

3. Morris, A.A.; Zhao, L.; Patel, R.S.; Jones, D.P.; Ahmed, Y., et al. Differences in systemic oxidative stress based on race and the metabolic syndrome: the morehouse and emory team up to eliminate health disparities (meta-health) study. *Metab. Syndr. Relat. Disord*. **2012**, *10*, 252–259;

4. Kander, M.C.; Cui, Y.; Liu, Z. Gender difference in oxidative stress: a new look at the mechanisms for cardiovascular diseases. *J. Cell. Mol. Med*. **2017**, *21*, 1024–1032;

5. Nuzzo, D.; Picone, P. Potential neurological effects of severe COVID-19 infection. *Neuroscience Research* **2020**, *158*, 1-5.

6. Nuzzo, D.; Vasto, S.; Scalisi, L.; Cottone, S.; Cambula, G.; Rizzo, M.; et al. Post-acute COVID-19 neurological syndrome: A new medical challenge. *J. Clin. Med.* **2021**, 10.

7. Narayanan, A.; Amaya, M.; Voss, K. Reactive oxygen species activate NFκB (p65) and p53 and induce apoptosis in RVFV infected liver cells. *Virology* **2014**, *449*, 270–286.

8. Nuzzo, D.; Cambula, G.; Bacile, I.; Rizzo, M.; Galia, M.; Mangiapane, P.; Picone, P.; Giacomazza, D.; Scalisi, L. Long-term brain disorders in post Covid-19 neurological syndrome (PCNS) patient. *Brain Sciences* **2021**, 11, 454.

9. Delgado-Roche, L.; Mesta, F. Oxidative stress as key player in severe acute respiratory syndrome coronavirus (SARS-CoV) infection. *Arch. Med. Res.* **2020**, *51*, 384–387.

10. WHO - COVID-19 vaccine tracker and landscape. 23 July **2021**. https://www.who.int/publications/m/item/draft-landscape-of-covid-19-candidate-vaccines.

11. Prasansuklab, A.; Theerasri, A.; Rangsinth, P.; Sillapachaiyaporn, C.; Chuchawankul, S.; Tencomnao, T. Anti-COVID-19 drug candidates: A review on potential biological activities of natural products in the management of new coronavirus infection. *J. Tradit. Complement. Med*. **2021**, *11*, 144–157.

12. Nuzzo, D.; Scordino, M.; Scurria, A.; Giardina C.; Giordano, F.; Meneguzzo F.; et al. Protective, Antioxidant and Antiproliferative Activity of Grapefruit IntegroPectin on SH-SY5Y Cells. International Journal of Molecular Sciences. **2021**, 22, 9368.

13. Nuzzo, D.; Presti, G.; Picone, P.; Galizzi, G.; Gulotta, E.; Giuliano, S.; Mannino, C.; et al. Effects of the aphanizomenon flos-aquae extract (Klamin®) on a neurodegeneration cellular model. *Oxidative medicine and cellular longevity* **2018**, 17, 2018:9089016.

14. Nuzzo, D.; Contardi, M.; Kossyvaki, D.; Picone, P.; Cristaldi, L.; Galizzi, G.; et al. Heat-resistant aphanizomenon flos-aquae (AFA) extract (Klamin®) as a functional ingredient in food strategy for prevention of oxidative stress. *Oxidative medicine and cellular longevity* **2019**, 11, 2019:9481390.

15. Giacomazza, D.; D'Andrea, D.; Provenzano, A.; Picone, P.; Provenzano, F.; et al. The precious content of the olive mill wastewater: the protective effect of the antioxidant fraction in cell cultures. *CyTA-Journal of Food* **2018**, 16 (1), 658-666

16. Jin, Z.; Du, X.; Xu, Y.; Deng, Y.; Liu, M.; Zhao, Y.; Zhang, B.; Li, X.; Zhang, L.; Peng, C.; et al. Structure of Mpro from SARS-CoV-2 and discovery of its inhibitors. *Nature* **2020**, *582*, 289–293.

17. Komura, M.; Suzuki, M.; Sangsriratanakul, N.; Ito, M.; Takahashi, S.; Alam, M.S.; Ono, M.; Daio, C.; Shoham, D.; Takehara, K. Inhibitory effect of grapefruit seed extract (GSE) on avian pathogens. *J Vet Med Sci.* **2019**, *30*, 466-472

18. Kang, S.T.; Son, H.K.; Lee, H.J.; Choi, J.S.; Choi, Y.I.; Lee, J.J. Effects of Grapefruit Seed Extract on Oxidative Stability and Quality Properties of Cured Chicken Breast. *Korean J Food Sci Anim Resour.* **2017**, *37*, 429-439.

19. Xu, W.T; Qu, W. Antibacterial effect of Grapefruit Seed Extract on food-borne pathogens and its application in the preservation of minimally processed vegetables. *Postharvest Biol. Technol.* **2007**, *45*, 126–133.

20. Lipiński, K.; Mazur, M.; Antoszkiewicz, Z.; Purwin, C. Polyphenols in monogastric nutrition - a review. *Ann. Anim. Sci.* **2017**, *17*, 41–58.

21. Reagor, L.; Gusman. J.; McCoy, L.; Carino, E.; Heggers, J.P. The effectiveness of processed grapefruit-seed extract as an antibacterial agent: I. An in vitro agar assay. *J Altern Complement Med*. **2002**, *8*, 325-32.

22. Heggers, J.P.; Cottingham, J.; Gusman, J.; Reagor, L.; McCoy, L.; Carino, E.; Cox, R.; Zhao, J.G. The effectiveness of processed grapefruit-seed extract as an antibacterial agent: II. Mechanism of action and in vitro toxicity. *J Altern Complement Med*. **2002**, *8*, 333-40.

23. Song, Y.J.; Yu, H.H.; Kim, Y.J.; Lee, N.K.; Paik, H.D. Anti-Biofilm Activity of Grapefruit Seed Extract against Staphylococcus aureus and Escherichia coli. *J Microbiol Biotechnol*. **2019,** *28*, 1177-1183.

24. Gori, A.; Boucherle, B.; Rey, A.; Rome, M.; Fuzzati, N.; Peuchmaur, M. Development of an innovative maceration technique to optimize extraction and phase partition of natural products. *Fitoterapia* **2021**, *148*.

25. Magurano, F.; Baggieri, M.; Marchi, A.; Rezza, G.; Nicoletti, L.; COVID-19 Study Group. SARS-CoV-2 infection: the environmental endurance of the virus can be influenced by the increase of temperature. *Clin Microbiol Infect*. **2021**, *27*, 289.e5-289.e7.

26. Torres-Valenzuela, L.S.; Ballesteros-Gómez, A.; Rubio, S. Green Solvents for the Extraction of High Added-Value Compounds from Agri-food Waste. *Food Eng. Rev.* **2020**, *12*, 83–100.

27. Anand, U.; Jakhmola, S.; Indari, O.; Jha, H.C.; Chen, Z.S.; Tripathi, V.; Pérez de la Lastra, J.M. Potential Therapeutic Targets and Vaccine Development for SARS-CoV-2/COVID-19 Pandemic Management: A Review on the Recent Update. *Front Immunol*. **2021**, *30*, 658519.

28. Abdulla, Z.A.; Al-Bashir, S.M.; Al-Salih, NS,.; Aldamen, A.A.; Abdulazeez, M.Z. A Summary of the SARS-CoV-2 Vaccines and Technologies Available or under Development. *Pathogens* **2021**, *22*.

29. Fan, S.; Zhang, C.; Luo, T.; Wang, J.; Tang, Y.; Chen, Z.; Yu, L. Limonin: A review of its pharmacology, toxicity, and pharmacokinetics. *Molecules* **2019**, *24*, 1–22.

30. Roy, A.; Saraf, S. Limonoids: Overview of significant bioactive triterpenes distributed in plants kingdom. *Biol. Pharm. Bull*. **2006**, *29*, 191–201.

31. Montoya, C.; González, L.; Pulido, S.; Atehortúa, L.; Robledo, S.M. Identification and quantification of limonoid aglycones content of Citrus seeds. *Rev. Bras. Farmacogn*. **2019**, 29, 710–714.

32. Yu, X.; Ding, G.; Zhi, X.; Xu, H. Insight into reduction of obacunone, and their ester derivatives as insecticidal agents against

Mythimna separata Walker. *Bioorganic Med. Chem. Lett.* **2015**, *25*, 25–29.

33. Battinelli, L.; Mengoni, F.; Lichtner, M.; Mazzanti, G.; Saija, A.; Mastroianni, C.M.; Vullo, V. Effect of Limonin and Nomilin on HIV-1 Replication on Infected Human Mononuclear Cells. *Planta Med*. **2003**, *69*, 910–913.

34. Shi, Y.S.; Zhang, Y.; Li, H.T.; Wu, C.H.; El-Seedi, H.R.; Ye, W.K.; Wang, Z.W.; Li, C. Bin; Zhang, X.F.; Kai, G.Y. Limonoids from Citrus: Chemistry, anti-tumor potential, and other bioactivities. *J. Funct. Foods* **2020**, *75*, 104213.

35. Kim, T.; Kim, J.H.; Oh, S.W. Grapefruit Seed Extract as a Natural Food Antimicrobial: a Review. *Food Bioprocess Technol*. **2021**, *14*, 626–633.

36. Vardhan, S.; Sahoo, S.K. In silico ADMET and molecular docking study on searching potential inhibitors from limonoids and triterpenoids for COVID-19. *Comput. Biol. Med*. **2020**, *124*, 103936.

Ringraziamenti

Per questo lavoro desidero ringraziare

- il Dott. Fabio Magurano e le dott.sse Melissa Baggieri, Antonella Marchi, Paola Bucci, Silvia Gioacchini, Giorgia Catinella, Gigliola Borgonovo per lo studio dell'attività antivirale su modelli cellulari;
- il Dott. Pasquale Picone e il Dott. Domenico Nuzzo per lo studio dello stress ossidativo su modelli cellulari ;
- la Prof.ssa Sabrina Dallavalle e il Prof. Andrea Pinto, per l'estrazione e la purificazione dei bioattivi;
- il Dottor Claudio Vernieri ed il Prof. Alessio Nencioni, che mi hanno supervisionato durante il mio dottorato.